Cell PRESS
Chemistry & Biology
Article

pHLIP-Mediated Translocation of Membrane-Impermeable Molecules into Cells

Damien Thévenin,[1] Ming An,[1] and Donald M. Engelman[1,*]
[1]Department of Molecular Biophysics and Biochemistry, Yale University, P.O. Box 208114, New Haven, CT 06520-8114, USA
*Correspondence: donald.engelman@yale.edu
DOI 10.1016/j.chembiol.2009.06.006

SUMMARY

Our goal is to define the properties of cell-impermeable cargo molecules that can be delivered into cells by pH (Low) Insertion Peptide (pHLIP), which can selectively target tumors in vivo based on their acidity. Using biophysical methods and fluorescence microscopy, we show that pHLIP can successfully deliver polar and membrane-impermeable cyclic peptides linked to its C terminus through the membranes of lipid vesicles and cancer cells. Our results also indicate that the translocation of these cargo molecules is pH dependent and mediated by transmembrane helix formation. Since a broad range of cell-impermeable molecules is excluded from discovery efforts because they cannot traverse membranes on their own, we believe that pHLIP has the potential to expand therapeutic options for acidic tissues such as tumors and sites of inflammation.

INTRODUCTION

Since many anticancer drugs have off-target side effects that severely limit the efficacy of chemotherapy (Fennelly, 1995; Ross and Small, 2002; Sehouli et al., 2002), the use of targeted drug delivery systems has emerged as a way to diminish such cytotoxic effects on healthy organs (Minko et al., 2004). Some, such as liposomes (Fenske and Cullis, 2005), polymers (Duncan, 2006; Haag and Kratz, 2006), and other nanoparticles (Torchilin, 2007; Yezhelyev et al., 2006), can passively target tumors due to the enhanced permeation and retention effect from the increased permeability and minimal lymphatic drainage of many solid tumors (Maeda et al., 2001; Maeda et al., 2000). However, this effect is small for certain tumors, including those that are preangiogenic, necrotic, or poorly vascularized (Allen and Cullis, 2004). Therefore, other specific targeting strategies have been developed, usually involving the addition of ligands that target a particular type of binding site on cancer cells. Most cancer cells overexpress certain receptors and enzymes (cancer biomarkers) due to the change in biology required for tumor progression (Hanrahan et al., 2005). For example, the receptors for luteinizing hormone-releasing hormone are overexpressed in breast, ovarian, and prostate cancer cells (Dharap and Minko, 2003; Dharap et al., 2003; Minko et al., 2004). Unfortunately, an important limitation of targeting specific binding sites is the heterogeneity of human tumors. Tumor cells are genetically and phenotypically complex, due in part to the accumulation of a large number of somatic mutations in the cancer genome and to the genetic variations in individual patients, so that only a subset of the cells in a tumor may be targeted and the rest continue to proliferate (Bild et al., 2006a, 2006b; Murphy et al., 2005). Cancer cells inside the same tumor or in different tumors from the same origin might then have different receptors on their surface. Thus, it may not be enough to rely on a single cancer biomarker even for one type of cancer or a single tumor, so it is important to ask which other features of tumors may be exploited for targeting.

Rapidly expanding cancer cells have abnormal nutritional requirements and metabolic traits, creating unique microenvironmental features that distinguish almost all malignant solid tumors from surrounding normal tissues. One such characteristic is the lower extracellular pH of tumors when compared with healthy tissues (pH 6.5–7.0 versus pH 7.2–7.4) (Cairns et al., 2006; Gerweck and Seetharaman, 1996). Acidosis results in part from the specially evolved metabolism of cancer cells, of which the most notable is the Warburg effect (i.e., the preference to use glycolysis to generate ATP, even in the presence of oxygen) (Kim and Dang, 2006), which leads to the accumulation of lactic acid in the cytoplasm and subsequent excretion of protons out of the cell. Other factors also contribute to extracellular acidity, such as the release of carbon dioxide from cancer cells (Helmlinger et al., 2002), poor clearance of extracellular protons by intratumor microvessels (Gatenby and Gillies, 2004), and induction of carbonic anhydrase IX in solid tumor tissues (Gatenby and Gillies, 2004; Swietach et al., 2007). For these reasons, acidosis is a hallmark of tumor progression from early to advanced stages and may provide an opportunity for tumor detection and targeted therapy (Junior et al., 2007; Mrkvan et al., 2005; Sethuraman et al., 2006).

Many pharmaceutical agents must reach specific organelles in the interior of the cell to exert their therapeutic action, e.g., agents of gene therapy need to reach the nucleus and proapoptotic anticancer drugs need access to mitochondria (Torchilin, 2008). However, the hydrophobic barrier of cell membranes prevents drug carriers from entering cells unless an active transport mechanism is involved. In a number of cases, the strategy is to rely on the endocytotic pathways to internalize the drug carrier and its payload. Various cell-penetrating proteins or peptides have shown the ability to deliver therapeutic agents into cells, with their cargo payload ranging from small molecules, peptides, and proteins to RNA and DNA polymers (Fischer et al., 2005; Futaki, 2006; Henriques et al., 2006; Martin and Rice, 2007; Wagstaff and Jans, 2006). Many of the these peptides contain fewer than 20 amino acids and are highly enriched in Arg or Lys, such

as TAT (Vives et al., 1997), penetratin (Derossi et al., 1994), pVEC (Elmquist et al., 2001), and other artificially designed peptides (Futaki et al., 2001). However, when taken up by some form of endocytosis, peptide drug conjugates and other delivery nanoparticles are still topologically outside of the cell, with endosomal membranes separating the cargo molecules from the cytoplasm. Thus, additional devices, such as GALA peptides or the N-terminal domain of the influenza virus hemagglutinin protein HA2 (Li et al., 2004; Stegmann, 2000), are used to facilitate the endosomal escape. These efforts highlight the need for delivery systems that directly transport drug molecules into the cell cytoplasm.

As an alternative, our method is based on pH (Low) Insertion Peptide (pHLIP), a peptide that inserts into lipid bilayers at acidic pH. Unlike other strategies, which may consist of a carrier component, a targeting agent, and an endosomal escape moiety, the pHLIP peptide can simultaneously target tumors, carry the cargo, and translocate the payload across the plasma membrane at low pH. pHLIP is a 36 amino acid peptide derived from the C helix of bacteriorhodopsin (Hunt et al., 1997). At pH above 7, pHLIP peptides are soluble as monomers in aqueous buffers and associate with lipid bilayer surfaces largely as unstructured peptides. Under acidic conditions, pHLIP inserts across a lipid bilayer with an apparent pK of 6 in vitro, forming a transmembrane helix (Hunt et al., 1997). The mechanism and thermodynamics of pHLIP-membrane interaction have been studied extensively (Hunt et al., 1997; Reshetnyak et al., 2008; Tang and Gai, 2008; Zoonens et al., 2008). At peptide concentrations below 7 μM, pHLIP is predominantly monomeric in all three states—in solution, on the membrane, and in the membrane (Reshetnyak et al., 2007). The pH-dependent insertion process is coupled to the protonation of one or both of the Asp residues located in the transmembrane region of the peptide (Hunt et al., 1997; Reshetnyak et al., 2006). Furthermore, pHLIP insertion seems to be reversible and unidirectional, with its C terminus translocated across the membrane (Reshetnyak et al., 2006, 2007). Once inserted, pHLIP helices cause minimal disturbance to phospholipid bilayers: they do not form pores or induce membrane permeabilization (Reshetnyak et al., 2006; Zoonens et al., 2008).

We have shown that pHLIP can accumulate and persist in vivo in tissues with mildly acidic environments (pH 6.5–7.0), including solid tumors in mice and inflammatory foci in rats. In comparison, pHLIP accumulation is much less favorable in healthy tissues, with their extracellular milieu at a physiological pH of 7.2–7.4. In a mouse breast adenocarcinoma model, fluorescently labeled pHLIP constructs found solid acidic tumors with a high degree of accuracy and accumulated in them, even at very early stages of tumor development (Andreev et al., 2007). In addition, pHLIP shows no toxicity to cells (Reshetnyak et al., 2006) or mice (Andreev et al., 2007) at concentrations tested (1–50 μM).

The insertion of pHLIP into lipid bilayers, leading to the formation of stable transmembrane helices, is associated with an energy release. We have established that this energy can be used to move cargo molecules across a membrane, raising the possibility of targeted drug delivery (Reshetnyak et al., 2006). It is also worth noting that pHLIP-mediated translocation of cargo molecules into cells is not mediated by endocytosis, interactions with cell surface receptors, or formation of pores in cell membranes (Reshetnyak et al., 2006).

However, there has not been any systematic exploration of the properties of cargo molecules that can be delivered. To this point we have only a scattering of data on the molecular characteristics that define what constitutes useable cargo molecules. Indeed, the properties of the cargos that have been previously shown to be translocated by pHLIP into the cytoplasm of cells were not well known or carefully controlled (Reshetnyak et al., 2006). For instance, when we described the phalloidin cargo as "cell impermeable" we neglected the presence of the Rhodamine (TRITC) moiety (octanol/water partition coefficient [Log $P_{o/w}$] = +2.9; molecular weight [MW] = 516) and the photocrosslinker (Log $P_{o/w}$ = +0.8; MW = 212, used to attached phalloidin-TRITC to pHLIP), resulting in a cargo molecule much less polar than the phalloidin alone, which has a Log $P_{o/w}$ of −2.9 (MW = 788). Similarly, the dansyl dye cargo has a calculated Log $P_{o/w}$ of +3, making it potentially cell permeable on its own.

The goal of the present study is to define the useful range of chemical properties for cargo molecules deliverable by pHLIP-mediated translocation. To accomplish this objective, we take advantage of the fact that a wide range of properties, such as polarity, charge, size, and shape, can be varied systematically in a host-guest model cyclic peptide. We show that pHLIP can successfully translocate cell-impermeable, polar cyclic peptides (Log $P_{o/w}$ = −3; MW ~800) through the membranes of lipid vesicles and cancer cells. Hence, we suggest that pHLIP can deliver membrane-impermeable molecules that are usually excluded from being tested as potential therapeutic agents, expanding the range of molecular alternatives.

RESULTS AND DISCUSSION

Design of Cargo Molecules

We chose cyclic hexapeptides as model cargo molecules in this study, to avoid ambiguities that might arise from alternative conformations that linear peptides might adopt in the various environments found in solution, at a membrane surface, or in a membrane interior. The cargo structures are shown in Figure 1A. These 7-nitrobenz-2-oxa-1,3-diazole (NBD)-cyclic-$(X)_4$ peptides ($NC(X)_4$) contain four X positions that are varied as Ser, Asp, Asn, or Arg residues, allowing adjustments of cargo polarity, as shown by their Log $P_{o/w}$ calculated using QikProp (Table 1). Overall, these cargo molecules were designed to be quite hydrophilic (Log $P_{o/w} < -2.5$), with the objective of making them membrane impermeable on their own. To follow the cargo and test for topology, we included a Lys residue carrying the NBD fluorescence probe, and to serve as the point of attachment to the carrier pHLIP peptide via a S-S disulfide bond we have an SH group.

The Designed Cargo Molecules are Membrane Impermeable

We used the dithionite ($S_2O_4^{-2}$) quenching of NBD fluorescence to confirm that the $NC(X)_4$ cargo peptides behave in accordance with our design and cannot cross a lipid bilayer on their own at the pH used to activate pHLIP translocation. For each cargo, NBD fluorescence was monitored at 530 nm (excited at 480 nm) when incubated with 1-palmitoyl-2-oleoyl-*sn*-glycero-3-phosphocholine (POPC) vesicles at pH 4.0. Figure 1B shows that addition of the membrane-impermeable dithionite ion leads to rapid, complete quenching of NBD fluorescence of all four

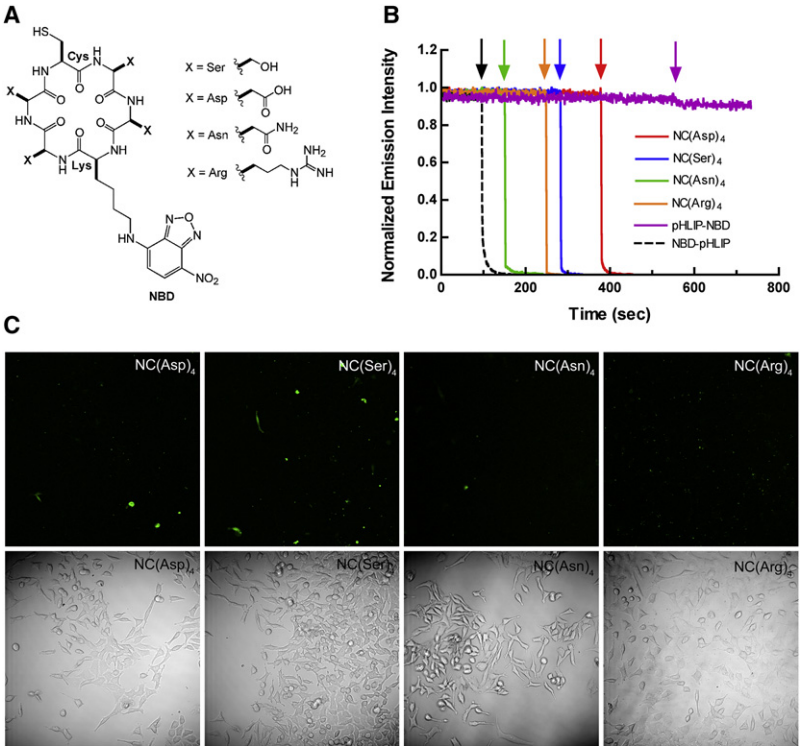

Figure 1. Cargo Peptides Do Not Cross Lipid Membrane on their Own

(A) Structures of the $NC(X)_4$ cargo peptides. The four peptides studied in this work, $NC(Ser)_4$, $NC(Asp)_4$, $NC(Asn)_4$, and $NC(Arg)_4$, follow the same model: four variable positions (X), a Cys residue for conjugation to pHLIP, and a NBD fluorescent probe attached to the side chain of a Lys residue.

(B) Dithionite quenching of NBD fluorescence signals of the $NC(X)_4$ cargo peptides (2 μM) not attached to pHLIP and of both N-terminal NBD-pHLIP and C-terminal pHLIP-NBD constructs (2 μM) in the presence of liposomes (peptide/lipid = 1:400) at pH 4.0. The arrows indicate the time of addition of dithionite. The circle indicates the first data point collected after the addition of dithionite.

(C) NBD fluorescence images of $NC(X)_4$ cargo peptides (5 μM) incubated with HeLa cells at pH 6.2 (top) and the corresponding phase-contrast images (bottom).

$NC(X)_4$ peptides, whereas no change of signal is observed when NBD is conjugated to the C terminus of pHLIP in the control construct pHLIP-NBD (100% protection). These results indicate that the C terminus of pHLIP is located inside the vesicles at pH 4, thus protecting NBD from dithionite quenching, while the $NC(X)_4$ cyclic cargo peptides stay outside. Slow quenching of NBD fluorescence is sometimes observed on a time scale of minutes, as can be seen for the pHLIP-NBD conjugate, perhaps due to leakage of dithionite or its decomposition products (Lem and Wayman, 1970; Wayman and Lem, 1970) into the liposomes at pH 4. As mentioned in the Experimental Procedures section, protection is evaluated from the first data point collected immediately after addition of dithionite (denoted by a circle in Figure 1B).

We also tested how $NC(X)_4$ peptides would behave in the presence of human cancer cells in an acidic environment by monitoring NBD fluorescence via confocal microscopy. Figure 1C shows that these cargo peptides do not cross the membrane of HeLa cells when incubated at pH 6.2. Indeed, with the exception of a few dead cells, no fluorescence is observed in the cytoplasm of the cells. Thus, these cargo molecules cannot cross a lipid bilayer or a cell membrane on their own.

Interactions of pHLIP-Cargo Constructs with Lipid Bilayers

Prior to evaluating pHLIP-mediated translocation of cyclic peptides into lipid vesicles and cancer cells, each $NC(X)_4$ cargo peptide was conjugated to the C terminus region of pHLIP-Cys via a disulfide bond. The interactions of these pHLIP-cargo constructs with lipid bilayers were then studied using circular dichroism (CD) and tryptophan fluorescence.

Far UV CD spectroscopy was used to determine the secondary structure of various pHLIP constructs in the presence of POPC liposomes at pH 8 and 4 (Figures 2A and 2B). Figure 2A shows that every pHLIP conjugate adopts an unstructured configuration at pH 8, whereas Figure 2B shows that all pHLIP conjugates form α helices under acidic conditions similar to that formed by pHLIP at pH 4, except for pHLIP-$NC(Arg)_4$. The latter remains unstructured when the pH is lowered from 8 to 4.

There are two Trp residues present in the sequence of pHLIP, and at least one of them is in the postulated transbilayer region of the peptide. Thus, since the Trp fluorescence emission is sensitive to the polarity of the environment, they serve as reporter groups for monitoring the interactions of pHLIP (or pHLIP conjugates) with lipid bilayers in POPC vesicles. At pH 8, the Trp fluorescence emission maxima of all pHLIP conjugates (except pHLIP-$NC(Arg)_4$) are centered around 350 nm (Figure 2C), reflecting the exposure of Trp residues to polar, aqueous environments (Burstein et al., 1973). Lowering the pH from 8 to 4 results in significant λ_{max} blue shifts ($\geq$10 nm, except for pHLIP-$NC(Arg)_4$) and increases in fluorescence intensity (except for pHLIP-$NC(Asn)_4$). These changes are characteristic for Trp residues buried in hydrophobic environments and suggest that at least pHLIP-$NC(Asp)_4$ and pHLIP-$NC(Ser)_4$ conjugates insert into vesicles at pH 4 (Burstein et al., 1973; Reshetnyak et al., 2007).

These findings agree with the pH-responsive changes in secondary structure revealed by CD. Taken together, notwithstanding the $NC(Arg)_4$ exception, these results indicate that conjugating a $NC(X)_4$ cargo peptide (or an NBD reporter group) to pHLIP does not disturb its characteristic shape-shifting behavior. Moreover, in very recent tryptophan fluorescence experiments, we measured the pK of insertion of pHLIP-$NC(Asp)_4$ into the bilayer of POPC vesicles to be 5.9 ± 0.1 (data not shown), which is very close to the value of 6.0 measured for pHLIP alone (Hunt et al., 1997). In other words, acidic environments can induce pHLIP conjugates to insert into lipid bilayers to form stable transmembrane α helices in a fashion similar to that of pHLIP.

Table 1. Properties of Cargo Molecules Attached to the C Terminus of pHLIP

C-Terminal Cargo	Log $P_{o/w}$ (Deprotonated)[a]	Log $P_{o/w}$ (Protonated)[a]	MW[a]
NBD	−0.83	−0.83	293.3
$NC(Ser)_4$	−2.68	−2.68	742.7
$NC(Asp)_4$	−11.92	−2.87	854.8
$NC(Asn)_4$	−8.52	−8.52	850.8
$NC(Arg)_4$	−4.34	−4.34	1025.2

[a] Log $P_{o/w}$ were calculated using QikProp 3.0 from the structures with deprotonated or protonated side chain carboxyl groups.

As observed in CD, pHLIP-$NC(Arg)_4$ does not behave like the other pHLIP conjugates: its Trp λ_{max} is already centered around 340 nm at pH 8 (Figure 2C), reflecting sequestration of Trp residues away from water—a state possibly mediated by aggregation. Furthermore, the Trp λ_{max} does not change significantly when the pH is lowered, which is consistent with the unstructured CD spectra observed at both pH 8 and 4 for this conjugate. In short, the pHLIP-$NC(Arg)_4$ construct seems to aggregate.

pHLIP-Mediated Translocation

We assessed the ability of pHLIP to translocate $NC(X)_4$ cargos across lipid bilayers and cell membranes. The conjugates were first tested with lipid vesicles. Figure 3A shows that when pHLIP-$NC(X)_4$ conjugates are incubated at pH 8 with POPC vesicles, addition of dithionite quenches NBD fluorescence in a rapid and complete fashion (0% protection) for all four pHLIP-$NC(X)_4$ conjugates, i.e., cargo molecules stay outside of the liposomes and are not translocated across lipid bilayers at neutral pH. However, when the pH is lowered to 4, different NBD fluorescence quenching traces are observed among the conjugates (Figure 3B). For pHLIP-$NC(Asn)_4$ and pHLIP-$NC(Arg)_4$ conjugates, NBD fluorescence is completely quenched by dithionite even at pH 4, with 0.4 ± 1.8% and 3 ± 5% protection observed, respectively (see Table 2), suggesting that these two conjugates leave their cargos outside of the liposomes under acidic conditions. In contrast, near complete protection from dithionite quenching is observed for pHLIP-NBD (91 ± 9%, positive control), pHLIP-$NC(Asp)_4$ (85 ± 7%), and pHLIP-$NC(Ser)_4$ (76 ± 8%) conjugates, showing that these three C-terminal cargos, with Log $P_{o/w}$ values in the range of −0.8 to −2.9, are successfully translocated into or across lipid bilayers by pHLIP. The quantitative results for these translocation assays are summarized in Table 2. As already shown in Figure 1B for pHLIP-NBD, slow quenching of NBD after addition of dithionite is also observed for pHLIP-$NC(Ser)_4$ and pHLIP-$NC(Asp)_4$, indicating that this effect is not specific to the $(Ser)_4$ and $(Asp)_4$ cargos and that these two cargos do not cause membrane distortion resulting in major liposome leakage.

We also evaluated the capability of pHLIP to deliver $NC(X)_4$ cargos across membranes and into the cytoplasm of HeLa cells using NBD fluorescence microscopy. The results are in complete agreement with that observed in liposomes. Figures 3C and 4 show that $NC(Asp)_4$ and $NC(Ser)_4$ cargos are translocated and released into cell cytoplasms (since the S-S bond that conjugates the cargo to pHLIP is cleaved in cells) only when the cells are incubated at pH 6.2. In contrast, pHLIP-$NC(Asn)_4$ and pHLIP-$NC(Arg)_4$ do not deliver their cargos into cell cytoplasms, regardless of the pH. In the case of pHLIP-$NC(Arg)_4$, the conjugate seems to stick to cell plasma membranes and aggregate on the glass window at both pHs, further confirming what we observed by CD (Figures 2A and 2B) and Trp fluorescence (Figure 2C). This behavior is perhaps caused by interactions between the multiple positive charges on the cargo peptide $NC(Arg)_4$ and the multiple negative charges on pHLIP (which has six carboxyl side chains) at neutral pH. In the case of pHLIP-$NC(Asn)_4$, we suggest that it is the polarity of the cargo (Log $P_{o/w}$ ∼−8.5) that prevents pHLIP constructs from inserting across lipid bilayers (at an appreciable rate), since its CD and Trp fluorescence data are consistent with the notion that this pHLIP conjugate undergoes a clear transition from random coil to helix when pH is decreased from 8 to 4. Furthermore, the pHLIP-$NC(Asn)_4$ construct seems to stick to the surface of HeLa cells at pH 6.2 as revealed by fluorescence microscopy (Figure 3C). Perhaps, this conjugate aggregates at or binds to the membrane surface as an α helix, as CD data suggest (Figure 2B). It is also interesting that even though $NC(Asp)_4$ is more hydrophilic than $NC(Asn)_4$ at neutral pH (calculated Log $P_{o/w}$ of −11.9 versus −8.5; see Table 1), the aspartic acid cargo is translocated into cells at pH 6.2 while the asparagine cargo is not, in agreement with what is observed in liposome quenching assays carried out at pH 4. Such behavior can be explained by the fact that the carboxylate side chains of $NC(Asp)_4$ can be protonated (by cell surface protons), leading to a significant decrease in cargo polarity (from a calculated Log $P_{o/w}$ of nearly −12 to −2.9), making the crossing of the hydrophobic bilayer interior less formidable. The local environment at the cell surface (i.e., the phospholipid head group region) could significantly increase the pKa of the carboxylate side chains of the Asp residue from its canonical values of ∼3.9, making the protonation more favorable at pH 6.2.

Moreover, even though $NC(Ser)_4$ and $NC(Asp)_4$ share similar Log $P_{o/w}$ values (about −3), they differ slightly in their molecular weights (742.7 versus 854.8, respectively), yet pHLIP translocates them with the same efficiency (76 ± 8% versus 85 ± 7%, respectively). This suggests that a Log $P_{o/w}$ of −3 (and MW of ∼850) may not represent absolute set limits and that pHLIP may be able to translocate even more polar or larger molecules.

Remarkably, the results obtained with the lipid vesicles correlate very well with that found in the presence of cancer cells. This finding supports the idea that liposomes are appropriate models to study pHLIP-mediated translocations in cells and that pHLIP peptides traverse cell membranes via direct insertion into the bilayer, reinforcing the view that pHLIP-assisted translocation is not mediated by membrane proteins or endocytosis.

SIGNIFICANCE

In conventional drug design aimed at intracellular targets, a constraint has been to create molecules that are sufficiently hydrophobic and/or small to traverse membranes on their own (Log $P_{o/w}$ from −0.4 to +5.6 and molecular weight [MW] of 160 to 480 g.mol^{-1}). As a result, cell-impermeable and larger molecules are usually excluded. Furthermore, many cancer drugs have off-target side effects that severely limit the efficacy of chemotherapy. In this work, we have

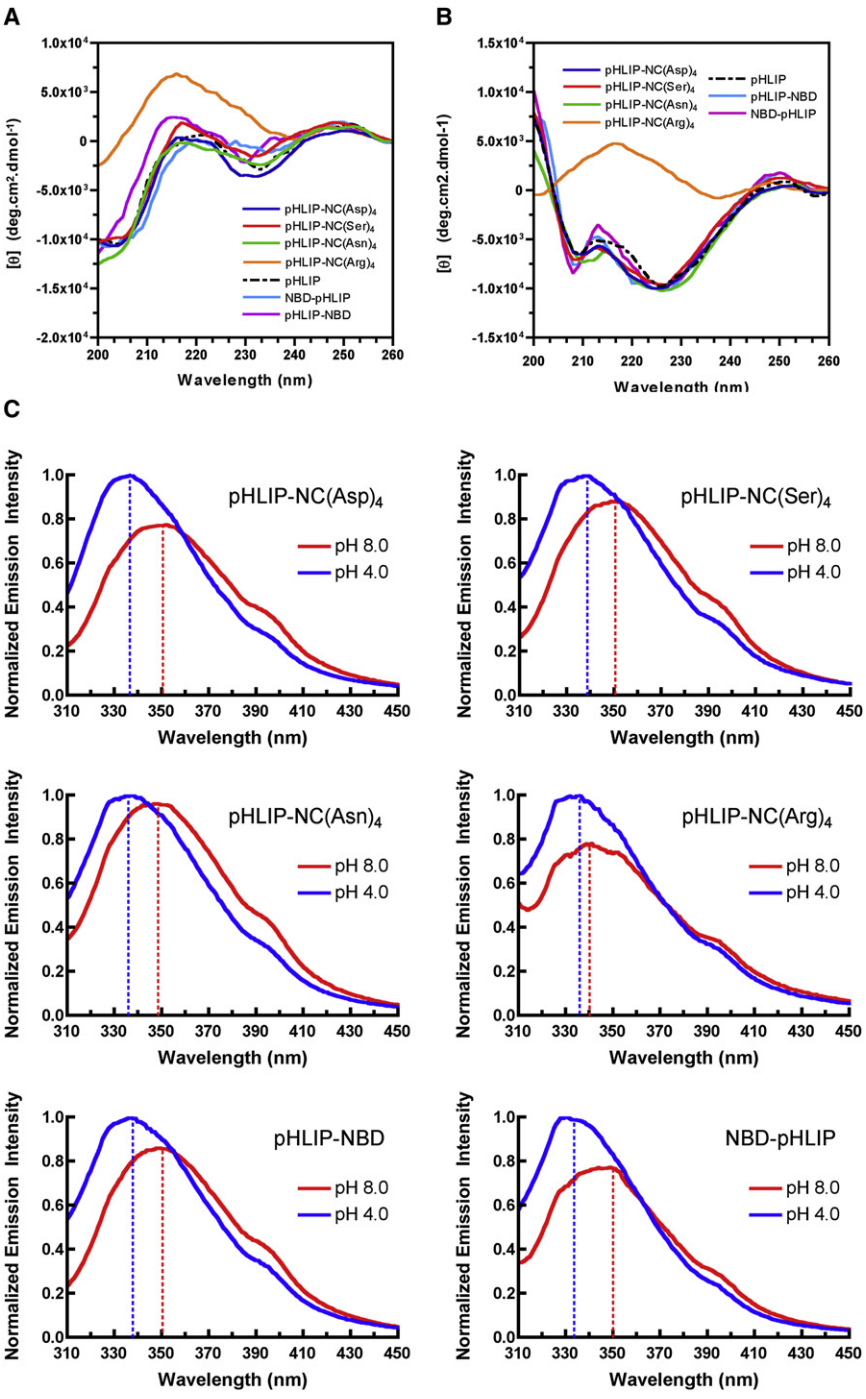

Figure 2. Interactions of pHLIP-Cargo Constructs with Lipid Bilayers

(A and B) CD spectra of pHLIP-cargo variants (7 μM) in the presence of POPC vesicles at pH 8.0 (A) and pH 4.0 (B).

(C) Tryptophan fluorescence spectra of pHLIP-cargo variants (2 μM) mixed in the presence of POPC vesicles at pH 8.0 (red spectra) and at pH 4.0 (blue spectra). The corresponding maxima of fluorescence emission are indicated by dotted lines.

explored the properties of pHLIP as a targeting and delivery system by defining some of the properties of molecules that can be translocated into cells; thus establishing boundary conditions for a new arena of drug design using this approach. Our method is based on pHLIP, a 36 amino acid peptide that is soluble at physiological pH and binds to membrane lipid bilayer surfaces if they are present. Unlike other strategies, it can simultaneously target tumors, carry the cargo, insert as a transmembrane helix, and translocate the payload across the plasma membrane at low pH. We find that cargo molecules with a Log $P_{o/w}$ of ~−3 and MW of ~800 are efficiently delivered into cancer cells. As a comparison, there is, to the best of our knowledge, no example of an existing anticancer drug with a Log $P_{o/w}$ < −1 and MW >500 that has intracellular targets. Thus, pHLIP may help to expand the chemical space for anticancer (and anti-inflammatory) drugs to include polar, cell-impermeable molecules aimed at cytoplasmic targets. Because such drug molecules will not easily cross cell membranes in normal tissues, certain side effects associated with conventional chemotherapy may also be mitigated.

EXPERIMENTAL PROCEDURES

Peptide Design and Synthesis

Two variants of pHLIP were used in this study: pHLIP-Cys with a cysteine residue at its C terminus and Cys-pHLIP with a cysteine at its N terminus. They have the following sequences: pHLIP-Cys, AAEQNPIYWARYADWLFTTPLLLLDLALLVDADEGTCG; Cys-pHLIP, ACEQNPIYWARYADWLFTTPLLLLDLALLVDADEGTG. Both variants were prepared by solid-phase peptide synthesis and purified via reverse-phase HPLC at the W.M. Keck Foundation Biotechnology Resource Laboratory (Yale University).

The cargo molecules are synthetic cyclic peptides following a host-guest model, called NBD-Cyclic-$(X)_4$ or $NC(X)_4$, where X is Arg, Asn, Asp, or Ser (Figure 1A). These cyclic hexapeptides also contain a Lys where the fluorescence probe NBD is attached and a Cys residue to allow conjugation to pHLIP via a disulfide bond. These cyclic peptides were purchased from Anaspec, Inc. and subsequently conjugated to pHLIP-Cys using methods described below. The Log $P_{o/w}$ of these cyclic cargo peptides was calculated using QikProp 3.0 (Schrödinger, LLC) for Windows (W. Jorgensen, Yale University) from the structures with deprotonated or protonated side chain carboxyl groups.

Syntheses of pHLIP Conjugates

Synthesis of pHLIP-S-S-NC(Ser)$_4$

Solvent mixture A consists of 1:1:3:5 of DMF, DMSO, methanol, and aqueous NH_4HCO_3 buffer (200 mM; pH 8). To a solution of TCEP.HCl (0.765 mg, 2.67 μmol, 3.38 eq.) in 85 μl of solvent mixture A was added a solution of

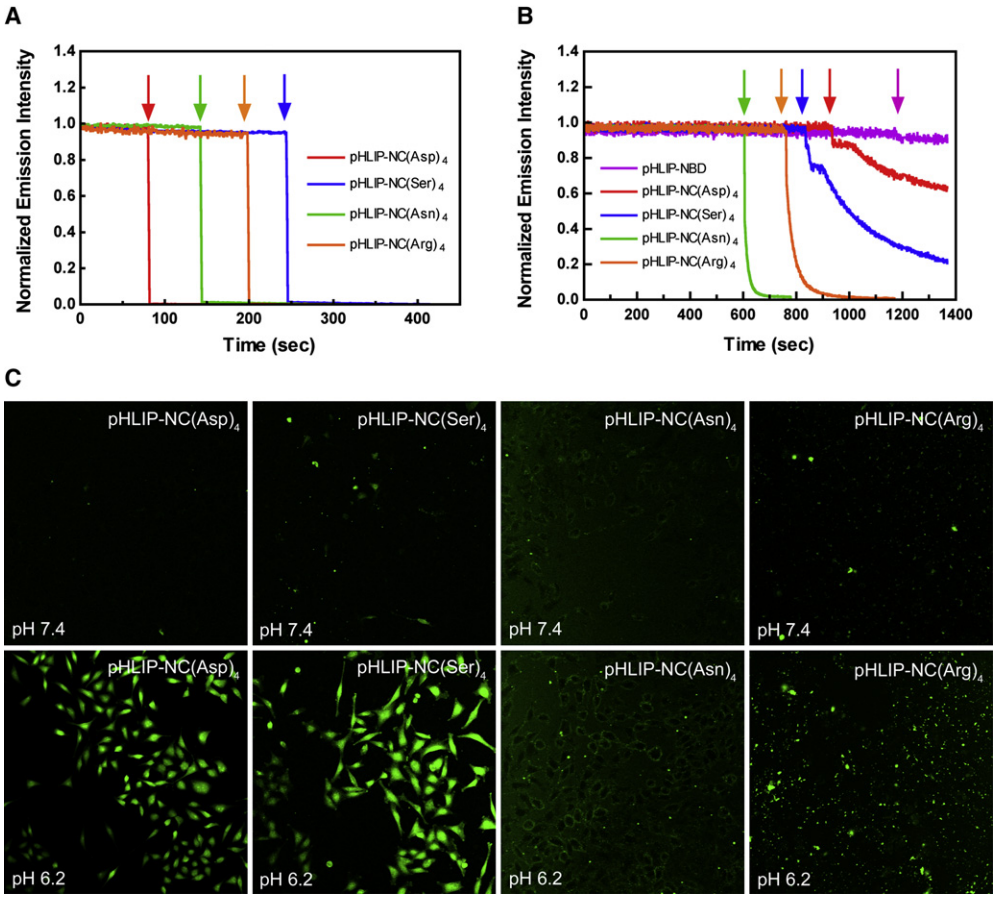

Figure 3. pHLIP Can Translocate Polar Molecules across Lipid Membrane

(A and B) Monitoring dithionite quenching of NBD fluorescence of pHLIP-NC(X)$_4$ constructs (2 μM) in the presence of liposomes at pH 8.0 (A) and pH 4.0 (B). The arrows indicate the time of addition of the quencher sodium dithionite. The circles indicate the first data point collected after the addition of dithionite.

(C) Monitoring pHLIP-mediated translocation of NC(X)$_4$ cargo peptides (5 μM) into HeLa cells at pH 7.4 (top panels) and pH 6.2 (bottom panels) by confocal microscopy.

cyclic peptide NC(Ser)$_4$ (0.585 mg, 0.79 μmol, 1 eq.) in 340 μl of A, followed by a solution of pHLIP-Cys (3.6 mg, 0.85 μmol, 1.08 eq.) in 340 μl of A. This mixture was stirred at room temperature and in the dark for 20 min. To this reduced mixture, an oxidizing solution of $K_3Fe(III)CN_6$ (6 mg, 18.2 μmol, 23.1 eq.) in 60 μl of aqueous NH_4HCO_3 buffer (200 mM; pH 8) was added. This reaction mixture was stirred at room temperature for 5 hr, and then allowed to sit at 0°C for 16 hr. The desired product was isolated via reverse-phase HPLC (Hewlett Packard Zorbax semi-prep 9.4 × 250 mm SB-C18 column; flow rate: 2 ml/min; phase A: water + 0.01% TFA; phase B: acetonitrile + 0.01% TFA; gradient: 70 min from 99:1 A/B to 1:99 A/B). Lyophilization provided the desired pHLIP-S-S-NC(Ser)$_4$ adduct (0.4 μmol) in ~50% yield. The product was quantified using UV-vis absorbance of the NBD group (ε 280 nm ~2,080 $M^{-1}cm^{-1}$, ε 348 nm ~9,800 $M^{-1}cm^{-1}$, ε 480 nm ~26,000 $M^{-1}cm^{-1}$) and pHLIP peptide (ε 280 nm ~13,940 $M^{-1}cm^{-1}$). MS (MALDI-TOF MS+): molecular weight calculated for pHLIP-S-S-NC(Ser)$_4$ ($C_{223}H_{329}N_{55}O_{71}S_2$): 4980.5. Found ($MH^+$): 4980.6.

Table 2. Percentage of Protection from Dithionite Quenching of NBD Fluorescence via pHLIP Insertion-Mediated Cargo Translocation into Liposomes at pH 4.0

C-Terminal Cargo	Percentage of Protection[a]	Log $P_{o/w}$ (pH 4.0)[b]	MW	Translocation
NBD	91 ± 9%	−0.83	293.3	✓
NC(Ser)$_4$	76 ± 8%	−2.68	742.7	✓
NC(Asp)$_4$	85 ± 7%	−2.87	854.8	✓
NC(Asn)$_4$	0.4 ± 1.8%	−8.52	850.8	X
NC(Arg)$_4$	3 ± 5%	−4.34	1025.2	X

[a] Percentage of Protection is given as mean ± SEM.

[b] Log $P_{o/w}$ at pH 4.0 is calculated from the fully protonated cyclic peptide structures.

Syntheses of pHLIP-S-S-NC(X)$_4$ Where X = Asp, Asn, or Arg

Other pHLIP-S-S-NC(X)$_4$ conjugates were prepared in similar fashions but often using a simplified, milder procedure in which the TCEP reduction step is omitted, thus allowing the use of less oxidizing reagent ($K_3Fe(III)CN_6$; 1–1.5 eq.). The desired adducts pHLIP-S-S-NC(X)$_4$ were isolated in 30%–40% yields. In the case of NC(Arg)$_4$, the reaction proceeded as a heterogeneous mixture (perhaps due to aggregation between the multiple positive charges on NC(Arg)$_4$ and the multiple negative charges on pHLIP). MS (MALDI-TOF MS+): molecular weight calculated for pHLIP-S-S-NC(Asp)$_4$ ($C_{227}H_{329}N_{55}O_{75}S_2$): 5092.5. Found ($MH^+$): 5100.6. Molecular weight calculated for pHLIP-S-S-NC(Asn)$_4$ ($C_{227}H_{333}N_{59}O_{71}S_2$): 5088.6. Found ($MH^+$): 5084.5.

Syntheses of C-Terminal pHLIP-NBD and N-Terminal NBD-pHLIP Adducts

To a solution of pHLIP-Cys (3 mg, 0.7 μmol, 1 eq.) or Cys-pHLIP in 900 μl of argon-saturated aqueous potassium phosphate buffer (100 mM; pH 7.25)

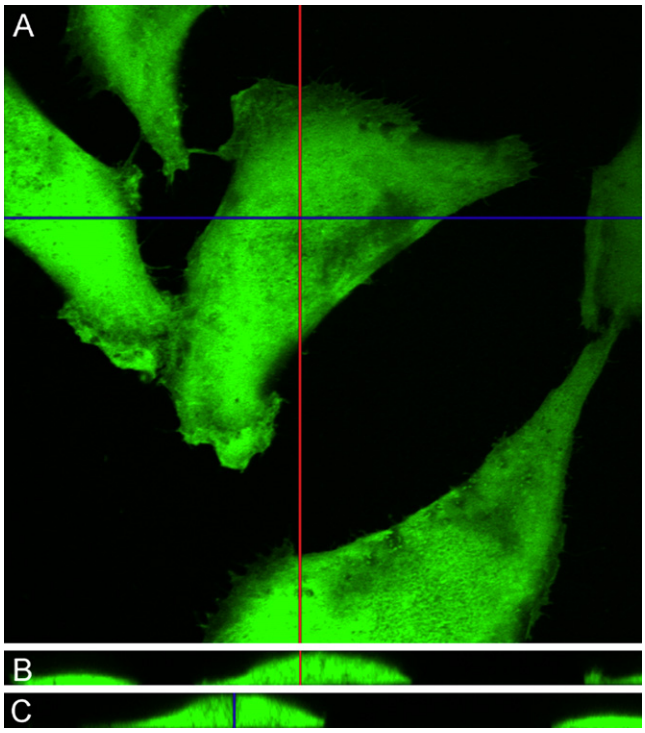

Figure 4. Representative Example of pHLIP-Assisted Translocation and Release of Cargo Molecules into the Cytoplasm of HeLa Cells
Confocal fluorescence microscopy images of pHLIP-NC(Asp)$_4$ (5 μM) incubated in the presence of HeLa cells at pH 6.2. Single projection of a z stack of 15 confocal sections (A), yz cross-section (red axis) (B), and xz cross-section (blue axis) (C).

was added a solution of IANBD amide (N,N'-dimethyl-N-(iodoacetyl)-N'-(7-nitrobenz-2-oxa-1,3-diazol-4-yl)ethylenediamine [Invitrogen]; 0.3 mg, 0.7 μmol, 1 eq.) in 300 μl of DMF. This reaction mixture was stirred at room temperature in the dark under argon for 20 hr. The desired adducts were isolated in >85% yield via C18 HPLC using methods described previously. The products were quantified using the 498 nm absorbance of the secondary amine NBD group (ε 498 nm ~23,500 $M^{-1}cm^{-1}$). MS (MALDI-TOF MS+): molecular weight calculated for pHLIP-NBD ($C_{208}H_{306}N_{50}O_{62}S$): 4531.0. Found ($MH^+$): 4531.4. Molecular weight calculated for NBD-pHLIP ($C_{205}H_{301}N_{49}O_{61}S$): 4459.9. Found ($MH^+$): 4460.6.

Liposome Preparation

Ten milligrams of POPC (Avanti Polar Lipids) in chloroform were dried under a stream of argon and then held under vacuum overnight. The dried lipid film was rehydrated with 1 ml of 100 mM sodium phosphate and 50 mM NaCl (buffer B) (pH 8.0) and vortexed. The resulting multilamellar vesicles were freeze-thawed in liquid nitrogen for seven cycles and were extruded through a polycarbonate membrane with 100 μm diameter pores using a mini extruder (Avanti Polar Lipids) to obtain unilamellar vesicles. Liposomes were used immediately following their preparation. Lipid concentration was checked using Marshall's assay (Stewart, 1980).

Sample Preparation for CD and Fluorescence Measurements

Prior to CD or fluorescence measurements, stock solutions of pHLIP constructs (0.2–0.5 mM) were prepared in acetonitrile/water (1:1). The concentration of the stock solution was determined by UV-vis absorption in 6 M guanidine-HCl (ε_{280} = 13,940 M^{-1} cm^{-1}; ε_{480} = 25,000 M^{-1} cm^{-1}). This stock solution was diluted to the working pHLIP concentration (of 2 or 7 μM) with buffer B and incubated overnight at room temperature in the dark. On the next day, when appropriate, solutions of POPC liposomes (prepared in buffer B) were added to the diluted pHLIP solution at a 1:400 peptide-to-lipid molar ratio and incubated for 3 hr at room temperature in the dark at pH 8.0. Subsequently, attempts at pHLIP insertion into the liposome lipid bilayer were triggered by reducing the pH from 8.0 to 4.0 with the addition of aliquots of a HCl solution. This mixture was allowed to equilibrate at pH 4 for 30 min prior to fluorescence and CD measurements.

Fluorescence Spectroscopy: Trp Fluorescence Measurements and NBD Fluorescence Quenching Assays

Measurements were carried out using a SLM-Aminco 8000C spectrofluorimeter (ISS) equipped with a thermo-bath RTE-111 (Neslab). All measurements were performed at 25°C and with pHLIP peptide concentrations equal to 2 μM. To minimize light scattering effects, the emission polarizer was oriented at 0° and the excitation polarizer at 90°. The widths of the emission and excitation slits were set to 4 nm. When tryptophan emission was monitored (pHLIP has two Trp residues), the samples were excited at 295 nm and the emission spectra were taken from 300 to 500 nm. When monitoring NBD fluorescence, the samples were excited at 480 nm and the fluorescence signal was monitored at 530 nm in slow kinetic mode.

pHLIP-mediated cargo translocation into liposomes was determined using the NBD-dithionite quenching reaction: membrane-impermeable dithionite ion ($S_2O_4^{2-}$) can chemically modify the NBD fluorophore and quench its fluorescence (McIntyre and Sleight, 1991). Changes in the fluorescence signal of NBD were monitored upon addition of 5 μl of sodium dithionite ($Na_2S_2O_4$) (pH 4.0; 1 M sodium phosphate; final dithionite concentration in the cuvette = 0.5–2 mM) to a 95 μl sample of pHLIP construct in buffer B that had been incubated in the presence of liposomes at pH 4.0 for 30 min. Fresh dithionite stock solution was prepared for each measurement because dithionite decomposes rapidly at low pH (Lem and Wayman, 1970; Wayman and Lem, 1970). The percentages of protection are calculated from the first data point collected after addition of dithionite.

CD Spectroscopy

Far UV CD spectra of pHLIP constructs were recorded on an Aviv model 215 spectrometer equipped with a Peltier thermal-controlled cuvette holder. All measurements were performed at 25°C and with pHLIP constructs prepared as mentioned above and at concentrations equal to 7 μM. CD intensities are expressed in mean residue molar ellipticity [θ] calculated from the following equation:

$$[\theta] = \frac{\theta_{obs}}{10.l.c.n} \left(\text{in degrees cm}^2.\text{dmol}^{-1}\right),$$

where θ_{obs} is the observed ellipticity in millidegrees, l is the optical path length in centimeters, c is the final molar concentration of the peptide, and n is the number of amino acid residues. Samples were measured in a 0.1 cm path length quartz cuvette and raw data were acquired from 260 nm to 190 nm at 1 nm intervals using a 2 s averaging time, and at least two scans were averaged for each sample.

Cancer Cell Assay and Confocal Fluorescence Microscopy

HeLa cells (kind gift from Dr. Mooseker, Yale University) were grown in 35-mm dishes with a 12-mm glass-bottom window (WillCo Wells) in DMEM supplemented with 10% FBS, 100 U/ml penicillin, and 0.1 mg/ml streptomycin in a humidified atmosphere of 5% CO_2 at 37°C. After 48 hr of culture, cells were washed twice with PBS buffer at the desired experimental pH and then incubated for 1 hr in PBS buffer at pH 7.4 or 6.2 in the presence of NC(X)$_4$ or pHLIP-S-S-NC(X)$_4$ (5 μM). After incubation, the cells were washed with PBS buffer at the experimental pH and fresh DMEM was then added. Fluorescent images were taken by using a Zeiss LSM 510 confocal microscope equipped with a 20× Plan-Apochromat (NA 0.8) objective and with excitation at 488 nm. A series of optical planes (z stack) were acquired using a 63× oil objective. Images were acquired by Zeiss ZEN software and processed using ImageJ (Abramoff et al., 2004) and the OrtView plug-in (MedNuc).

ACKNOWLEDGMENTS

The authors thank Mark S. Mooseker and Joseph Wolenski (Department of Molecular, Cellular and Developmental Biology, Yale University) for the kind

gift of HeLa cells and help with confocal microscopy, respectively. We also would like to thank Yana K. Reshetnyak and Oleg A. Andreev (Physics Department, University of Rhode Island) for their insights and comments. This work was supported by National Institutes of Health grants GM073857 and CA133890 and by an Anna Fuller Fellowship to M.A.

Received: March 20, 2009
Revised: May 8, 2009
Accepted: June 9, 2009
Published: July 30, 2009

REFERENCES

Abramoff, M.D., Magelhaes, P.J., and Ram, S.J. (2004). Image processing with ImageJ. Biophotonics International *11*, 36–42.

Allen, T.M., and Cullis, P.R. (2004). Drug delivery systems: entering the mainstream. Science *303*, 1818–1822.

Andreev, O.A., Dupuy, A.D., Segala, M., Sandugu, S., Serra, D.A., Chichester, C.O., Engelman, D.M., and Reshetnyak, Y.K. (2007). Mechanism and uses of a membrane peptide that targets tumors and other acidic tissues in vivo. Proc. Natl. Acad. Sci. USA *104*, 7893–7898.

Bild, A.H., Potti, A., and Nevins, J.R. (2006a). Linking oncogenic pathways with therapeutic opportunities. Nat. Rev. Cancer *6*, 735–741.

Bild, A.H., Yao, G., Chang, J.T., Wang, Q., Potti, A., Chasse, D., Joshi, M.B., Harpole, D., Lancaster, J.M., Berchuck, A., et al. (2006b). Oncogenic pathway signatures in human cancers as a guide to targeted therapies. Nature *439*, 353–357.

Burstein, E.A., Vedenkina, N.S., and Ivkova, M.N. (1973). Fluorescence and the location of tryptophan residues in protein molecules. Photochem. Photobiol. *18*, 263–279.

Cairns, R., Papandreou, I., and Denko, N. (2006). Overcoming physiologic barriers to cancer treatment by molecularly targeting the tumor microenvironment. Mol. Cancer Res. *4*, 61–70.

Derossi, D., Joliot, A.H., Chassaing, G., and Prochiantz, A. (1994). The third helix of the Antennapedia homeodomain translocates through biological membranes. J. Biol. Chem. *269*, 10444–10450.

Dharap, S.S., and Minko, T. (2003). Targeted proapoptotic LHRH-BH3 peptide. Pharm. Res. *20*, 889–896.

Dharap, S.S., Qiu, B., Williams, G.C., Sinko, P., Stein, S., and Minko, T. (2003). Molecular targeting of drug delivery systems to ovarian cancer by BH3 and LHRH peptides. J. Control. Release *91*, 61–73.

Duncan, R. (2006). Polymer conjugates as anticancer nanomedicines. Nat. Rev. Cancer *6*, 688–701.

Elmquist, A., Lindgren, M., Bartfai, T., and Langel, U. (2001). VE-cadherin-derived cell-penetrating peptide, pVEC, with carrier functions. Exp. Cell Res. *269*, 237–244.

Fennelly, D. (1995). Dose intensity in advanced ovarian cancer: have we answered the question? Clin. Cancer Res. *1*, 575–582.

Fenske, D.B., and Cullis, P.R. (2005). Entrapment of small molecules and nucleic acid-based drugs in liposomes. Methods Enzymol. *391*, 7–40.

Fischer, R., Fotin-Mleczek, M., Hufnagel, H., and Brock, R. (2005). Break on through to the other side-biophysics and cell biology shed light on cell-penetrating peptides. ChemBioChem *6*, 2126–2142.

Futaki, S. (2006). Oligoarginine vectors for intracellular delivery: design and cellular-uptake mechanisms. Biopolymers *84*, 241–249.

Futaki, S., Suzuki, T., Ohashi, W., Yagami, T., Tanaka, S., Ueda, K., and Sugiura, Y. (2001). Arginine-rich peptides. An abundant source of membrane-permeable peptides having potential as carriers for intracellular protein delivery. J. Biol. Chem. *276*, 5836–5840.

Gatenby, R.A., and Gillies, R.J. (2004). Why do cancers have high aerobic glycolysis? Nat. Rev. Cancer *4*, 891–899.

Gerweck, L.E., and Seetharaman, K. (1996). Cellular pH gradient in tumor versus normal tissue: potential exploitation for the treatment of cancer. Cancer Res. *56*, 1194–1198.

Haag, R., and Kratz, F. (2006). Polymer therapeutics: concepts and applications. Angew. Chem. Int. Ed. Engl. *45*, 1198–1215.

Hanrahan, E.O., Hennessy, B.T., and Valero, V. (2005). Neoadjuvant systemic therapy for breast cancer: an overview and review of recent clinical trials. Expert Opin. Pharmacother. *6*, 1477–1491.

Helmlinger, G., Sckell, A., Dellian, M., Forbes, N.S., and Jain, R.K. (2002). Acid production in glycolysis-impaired tumors provides new insights into tumor metabolism. Clin. Cancer Res. *8*, 1284–1291.

Henriques, S.T., Melo, M.N., and Castanho, M.A.R.B. (2006). Cell-penetrating peptides and antimicrobial peptides: how different are they? Biochem. J. *399*, 1–7.

Hunt, J.F., Earnest, T.N., Bousché, O., Kalghatgi, K., Reilly, K., Horváth, C., Rothschild, K.J., and Engelman, D.M. (1997). A biophysical study of integral membrane protein folding. Biochemistry *36*, 15156–15176.

Junior, A.D., Mota, L.G., Nunan, E.A., Wainstein, A.J., Wainstein, A.P., Leal, A.S., Cardoso, V.N., and De Oliveira, M.C. (2007). Tissue distribution evaluation of stealth pH-sensitive liposomal cisplatin versus free cisplatin in Ehrlich tumor-bearing mice. Life Sci. *80*, 659–664.

Kim, J.W., and Dang, C.V. (2006). Cancer's molecular sweet tooth and the Warburg effect. Cancer Res. *66*, 8927–8930.

Lem, W.J., and Wayman, M. (1970). Decomposition of aqueous dithionite. Part I. Kinetics of decomposition of aqueous sodium dithionite. Can. J. Chem. *48*, 776–781.

Li, W., Nicol, F., and Szoka, F.C., Jr. (2004). GALA: a designed synthetic pH-responsive amphipathic peptide with applications in drug and gene delivery. Adv. Drug Deliv. Rev. *56*, 967–985.

Maeda, H., Wu, J., Sawa, T., Matsumura, Y., and Hori, K. (2000). Tumor vascular permeability and the EPR effect in macromolecular therapeutics: a review. J. Control. Release *65*, 271–284.

Maeda, H., Sawa, T., and Konno, T. (2001). Mechanism of tumor-targeted delivery of macromolecular drugs, including the EPR effect in solid tumor and clinical overview of the prototype polymeric drug SMANCS. J. Control. Release *74*, 47–61.

Martin, M.E., and Rice, K.G. (2007). Peptide-guided gene delivery. AAPS J. *9*, E18–E29.

McIntyre, J.C., and Sleight, R.G. (1991). Fluorescence assay for phospholipid membrane asymmetry. Biochemistry *30*, 11819–11827.

Minko, T., Dharap, S.S., Pakunlu, R.I., and Wang, Y. (2004). Molecular targeting of drug delivery systems to cancer. Curr. Drug Targets *5*, 389–406.

Mrkvan, T., Sirova, M., Etrych, T., Chytil, P., Strohalm, J., Plocova, D., Ulbrich, K., and Rihova, B. (2005). Chemotherapy based on HPMA copolymer conjugates with pH-controlled release of doxorubicin triggers anti-tumor immunity. J. Control. Release *110*, 119–129.

Murphy, N., Millar, E., and Lee, C.S. (2005). Gene expression profiling in breast cancer: towards individualising patient management. Pathology *37*, 271–277.

Reshetnyak, Y.K., Andreev, O.A., Lehnert, U., and Engelman, D.M. (2006). Translocation of molecules into cells by pH-dependent insertion of a transmembrane helix. Proc. Natl. Acad. Sci. USA *103*, 6460–6465.

Reshetnyak, Y.K., Segala, M., Andreev, O.A., and Engelman, D.M. (2007). A monomeric membrane peptide that lives in three worlds: in solution, attached to, and inserted across lipid bilayers. Biophys. J. *93*, 2363–2372.

Reshetnyak, Y.K., Andreev, O.A., Segala, M., Markin, V.S., and Engelman, D.M. (2008). Energetics of peptide (pHLIP) binding to and folding across a lipid bilayer membrane. Proc. Natl. Acad. Sci. USA *105*, 15340–15345.

Ross, R.W., and Small, E.J. (2002). Osteoporosis in men treated with androgen deprivation therapy for prostate cancer. J. Urol. *167*, 1952–1956.

Sehouli, J., Stengel, D., Elling, D., Ortmann, O., Blohmer, J., Riess, H., Lichtenegger, W., and Ovarian Cancer Study Group of the Nordostdeutsche Gesellschaft für Gynäkologische Onkologie (NOGGO). (2002). First-line chemotherapy with weekly paclitaxel and carboplatin for advanced ovarian cancer: a phase I study. Gynecol. Oncol. *85*, 321–326.

Sethuraman, V.A., Na, K., and Bae, Y.H. (2006). pH-responsive sulfonamide/PEI system for tumor specific gene delivery: an in vitro study. Biomacromolecules *7*, 64–70.

Stegmann, T. (2000). Membrane fusion mechanisms: the influenza hemagglutinin paradigm and its implications for intracellular fusion. Traffic *1*, 598–604.

Stewart, J.C. (1980). Colorimetric determination of phospholipids with ammonium ferrothiocyanate. Anal. Biochem. *104*, 10–14.

Swietach, P., Vaughan-Jones, R.D., and Harris, A.L. (2007). Regulation of tumor pH and the role of carbonic anhydrase 9. Cancer Metastasis Rev. *26*, 299–310.

Tang, J., and Gai, F. (2008). Dissecting the membrane binding and insertion kinetics of a pHLIP peptide. Biochemistry *47*, 8250–8252.

Torchilin, V.P. (2007). Targeted pharmaceutical nanocarriers for cancer therapy and imaging. AAPS J. *9*, E128–E147.

Torchilin, V.P. (2008). Tat peptide-mediated intracellular delivery of pharmaceutical nanocarriers. Adv. Drug Deliv. Rev. *60*, 548–558.

Vives, E., Brodin, P., and Lebleu, B. (1997). A truncated HIV-1 Tat protein basic domain rapidly translocates through the plasma membrane and accumulates in the cell nucleus. J. Biol. Chem. *272*, 16010–16017.

Wagstaff, K.M., and Jans, D.A. (2006). Protein transduction: cell penetrating peptides and their therapeutic applications. Curr. Med. Chem. *13*, 1371–1387.

Wayman, M., and Lem, W.J. (1970). Decomposition of aqueous dithionite. Part II. A reaction mchanism for decomposition of aqueous sodium dithionite. Can. J. Chem. *48*, 782–787.

Yezhelyev, M.V., Gao, X., Xing, Y., Al-Hajj, A., Nie, S.M., and O'Regan, R.M. (2006). Emerging use of nanoparticles in diagnosis and treatment of breast cancer. Lancet Oncol. *7*, 657–667.

Zoonens, M., Reshetnyak, Y.K., and Engelman, D.M. (2008). Bilayer interactions of pHLIP, a peptide that can deliver drugs and target tumors. Biophys. J. *95*, 225–235.

